Experimental Analysis of the Interaction Between a Dual-Bell Nozzle with an External Flow Field Aft of a Backward-Facing Step

Istvan Bolgar(✉), Sven Scharnowski, and Christian J. Kähler

Institute of Fluid Mechanics and Aerodynamics, Bundeswehr University Munich, Werner-Heisenberg-Weg 39, 85577 Neubiberg, Germany
istvan.bolgar@unibw.de
https://www.unibw.de/lrt7-en/team/istvan-bolgar

Abstract. Previous research on Dual-Bell nozzle flow always neglected the influence of the outer flow on the nozzle flow and its transition from sea level to altitude mode. Therefore, experimental measurements on a Dual-Bell nozzle with trans- ($Ma_\infty = 0.8$) and a supersonic ($Ma_\infty = 1.6$ & 2.0) external flows about a launcher-like forebody were carried out in the Trisonic Wind Tunnel Munich with particle image velocimetry and the schlieren technique. The sea level mode was investigated in transonic conditions, whereas transition and the altitude mode took place in supersonic conditions. The results show that there is a strong interaction between the nozzle flow and the outer flow in sea level mode, highly dominated by screeching. In contrast, there is no apparent correlation between the nozzle flow and the outer flow in the altitude mode. Transition from sea level to altitude mode shows multiple retransitions over a wide range of nozzle pressure ratios. This is due to an interaction of the nozzle flow with a supersonic expansion about the nozzle's lip. For the feasibility of the Dual-Bell concept, future research should investigate if a transition in transonic free-stream conditions is possible without the flip-flop effect.

Keywords: Dual-Bell nozzle · Shear layer · Particle image velocimetry

1 Introduction

The Ariane 5 space laucnher has a geometric discontinuity, similar to a BFS, at the end of its main stage ahead of the cryogenic engine. This causes the flow to separate from the main body, building up a turbulent shear layer. The shear layer reattaches onto the nozzle of the main engine with strong local pressure fluctuations [1]. This can lead to the excitement of structural modes of the main engine's nozzle, a phenomenon termed buffeting, which can cause catastrophic structural damage.

On a planar BFS the authors showed that the so-called 'step mode' is mainly responsible for the pressure fluctuations imposed on the reattachment surface [2].

A. Dillmann et al. (Eds.): DGLR 2018, NNFM 142, pp. 405–415, 2020.
https://doi.org/10.1007/978-3-030-25253-3_39

By applying passive flow control, the root mean square (RMS) of the pressure fluctuations was reduced by 50% [3]. This load reduction is achieved by so-called 'lobes' creating strong streamwise vorticity aft of the BFS, and thereby diffusing the critical step mode. Furthermore, these lobes reduced the mean reattachment length by more than 80%, thereby decreasing the moment arm of the pressure fluctuations. This large reduction in the dynamic moment of force makes adaptive nozzle concepts, which usually are longer and heavier, a feasible option for increasing the performance of current space launchers.

Recently, a publication showed that a change from the currently used nozzle on Ariane 5 to a so-called 'Dual-Bell' nozzle would yield a 490 kg increase in its payload capacity on a typical geostationary transfer orbit mission [4]. The Dual-Bell concept first appeared in literature in 1949 [5]. This nozzle features two consecutive divergent sections. The first section expands the flow into sea level mode, where the flow ideally is separated at a sharp edge at the end of the first Bell. In order to increase the thrust at altitude, a second Bell allows the flow to expand further into altitude mode, as soon as the surrounding ambient pressure decreases below a certain value. This so-called transition ideally has to occur instantly without re-transitioning back to sea level mode. Transition has been a major research focus in for two decades [6–10]. Some of these experiments also tried imposed external pressure fluctuations numerically or experimentally via a altitude chamber. However, the interaction of the external flow with the nozzle flow has always been neglected. Therefore it is the aim of the current research to characterize severity of these effects.

2 Experimental Setup

The experiments under investigation were conducted in the Trisonic Wind Tunnel Munich (TWM) at the Bundeswehr University Munich, which is a two-throat blow-down type wind tunnel with test section dimensions of 300 mm in width and 675 mm in height. It has an operating total pressure range of 1.2–5 bar and a Mach number range of 0.15–3.00. For the transonic measurements, the side/vertical wall suction capability of the TWM was applied. This not only helps in reducing the low momentum boundary layers on the side walls of the test section, but also reduces blockage effects at transonic conditions. Additionally for all Mach numbers, the horizontal walls were put at a deflection angle, increasing the cross section in the direction of the flow by 25 mm over the test section length of 1.8 m, in order to offset the increasing displacement thickness of the boundary layer on the horizontal walls, thereby decreasing the effect on the pressure gradient in the test section. Table 1 provides an overview of the experimental conditions. The ± values in the table indicate the standard deviation of each quantity during the measurements, while the measurement uncertainty is within ±1%. The nozzle's settling chamber pressure for the different measurements is provided in the last column and is denoted by $p_{n,0}$ In order to achieve transition of the nozzle at $Ma_\infty = 1.6$, the total pressure in the test section was linearly reduced from 4.3 bar to 3.6 bar in 4 s while keeping the nozzle chamber pressure constant to 4 bar. For more details about the measurement facility the reader is referred to [2].

Table 1. Free-stream flow conditions of TWM for experiments under investigation

Ma_∞	p_0 [bar]	p_∞ [bar]	T_0 [K]	U_∞ [$\frac{\mathrm{m}}{\mathrm{s}}$]	$p_{n,0}$ [bar]
0.80 ± 0.0008	1.30 ± 0.0013	0.852 ± 0.0008	291 ± 1.2	259	5.95 ± 0.05
1.60 ± 0.0050	4.3 to 3.6 in 4 s	1.01 to 0.85 in 4 s	292 ± 1.5	446	3.95 ± 0.05
2.00 ± 0.0010	2.50 ± 0.0022	0.320 ± 0.0004	292 ± 1.6	509	5.95 ± 0.05

2.1 BFS Model

The BFS model is symmetric about its horizontal plane and spans across the entire test section horizontally. It has a gently curved nose, in order to ensure subsonic conditions locally (at $Ma_\infty = 0.80$) [11], which then smoothly transitions into a flat plate. The model's length prior to the step is 252.5 mm, with 102.5 mm of that being the flat plate. The step then has a height of $h = 5$ mm and attaches to a splitter plate, which also serves as the nozzle fairing, with a length of 35 mm. The step height to step width ratio is 1 : 40, which provides for an unaffected recirculation region due to side wall effects [12]. The overall model's thickness is 25 mm, or 3.7% of the test section's height. At the center of the splitter plate with a height of 15 mm, a 2D Dual-Bell nozzle with a nozzle exit height of 14 mm spans 56 mm across the model. The first extension of the Dual-Bell nozzle is a truncated ideal contour (TIC), while the second extension of the Dual-Bell is a constant pressure contour. The nozzle throat is 2.61 mm in height, giving it an expansion ratio of $\epsilon = 5.36$, resulting in a design exit Mach number of 3.29. The thrust chamber is fed by two 2″ hoses, one on either side of the model (refer to Fig. 1), with the thrust chamber/model being symmetric about its horizontal and streamwise vertical planes. For the experiments under investigation the nozzle settling chamber pressure was set at 6 bar for the steady state experiments, and 4 bar for the transient experiment in order to achieve transition.

2.2 Particle Image Velocimetry

Particle image velocimetry (PIV) was used to capture instantaneous flow fields in a streamwise vertical field of view (FOV). The light source was a Quantel EverGreen double pulse laser with 200 mJ per pulse. The light illuminated Di-Ethyl-Hexyl-Sebacat (DEHS) tracer particles with a mean diameter of 1 µm [13]. The particles were added far upstream of the test section for a homogeneous particle distribution. A 50 mm planar objective lens from Zeiss imaged the particles onto a 2560×2160 pixel sensor of a LaVision Imager sCMOS camera. The synchronous triggering of the light source and the camera was managed by a LaVision PTU X. For each test case, 500 double images with a statistically independent frequency of 15 Hz were recorded. The time separation between an image pair was 1.0 µs, limiting the particle image shift to about $10 - 15$ pixel in the nozzle flow. This ensures that the error due to curved streamlines and spatial gradients, which lead to loss-of-correlation due to out-of-plane motion, is sufficiently low [14,15]. For the data processing, a pre-processing step was comprised

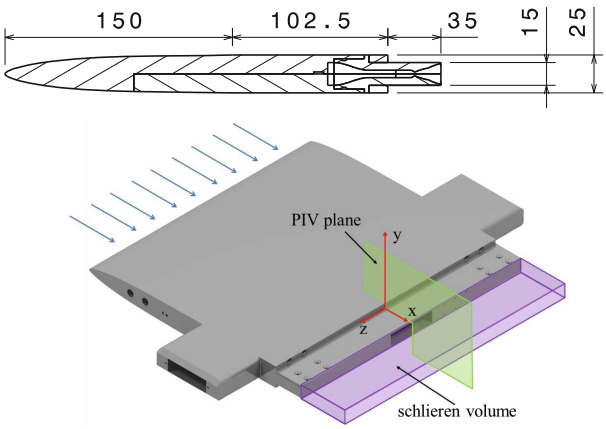

Fig. 1. Top: Dimensional cut-view of the 2D Dual-Bell launcher model; Bottom: Illustration of the launcher model with its measurement locations for PIV and schlieren

of an image shift correction in order to compensate for camera vibrations, and subtracting the background reflections by means of proper orthogonal decomposition (POD) [16]. The final interrogation window size of the PIV evaluation was 12×12 pixel with 50% overlap, yielding a vector grid spacing of approximately 285 µm. The PIV evaluation included a Gaussian window weighting and image deformation as implemented in the LaVision DaVis 8.3 software. Statistical flow field data was obtained by extracting the necessary information from the resulting instantaneous vector fields.

2.3 Schlieren Measurements

For further analyses regarding the transitional behavior of the nozzle, a four color schlieren system was used, which allows the visualization of density gradients, isentropic compression and expansion waves, and compressible shear layers. The extracted colors were red, green, blue and yellow. The light was focused onto a high-speed camera sensor recording at 20 kHz. For a detailed description of the schlieren system installed at the TWM facility, the reader is referred to [2,17].

3 Results

3.1 Sea Level Mode

The sea level mode was investigated at a nozzle pressure ratio ($NPR = p_{0_{nozzle}}/p_\infty$) of 7. In Fig. 2 one can see that a reverse flow region develops in the second extension of the nozzle. This is to be expected, as the second extension of the bell is not filled in sea level mode. One of the streamlines from the outer flow extends into the nozzle, indicating that an interaction may be present.

For a more detailed statistical analysis, the fluctuating component of the vertical velocity scalar v' at a location close to the nozzle exit was correlated with itself in the entire 2D FOV (refer to [18] for the definition of Pearson's correlation coefficient). Figure 3 shows the resulting correlation in the 2D FOV, where strong correlations and anti-correlations are present throughout the entire flow field. Thus, a strong interaction is present at the nozzle exit with the rest of the flow field. The correlations are noticeably periodically organized and aligned with an angle and shape that closely resembles shocks. Therefore, these shock-like structures were searched for in the instantaneous vector fields in the next step.

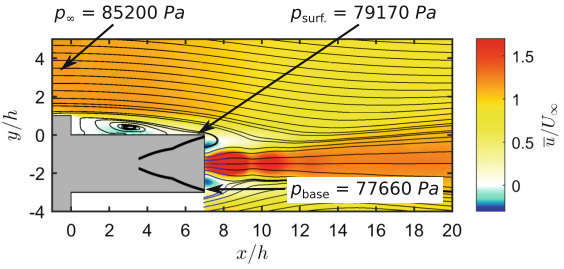

Fig. 2. Illustration of the streamwise component of the mean flow field at $Ma_\infty = 0.8$ and $NPR = 7$

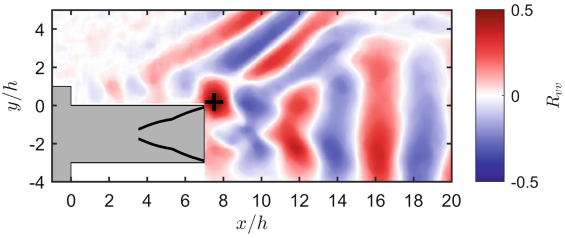

Fig. 3. Illustration of a two-point correlation of v' at $Ma_\infty = 0.8$ with $= 7$

A set of two instantaneous vector fields at the previously described experimental conditions is shown in Fig. 4. The shock-like structures are present in the temporal snap shots as well. The way that these waves are developing after one another, as well as their shape and angle, very closely resemble that what has been defined to be nozzle screeching in literature [19,20]. Nozzle screeching has mostly been observed in nozzle flows without an outer flow. At that point, screeching can be seen in schlieren photographs as weak acoustic sound waves. However, when an external flow close to sonic conditions is superimposed on these sound waves, the combination leads to shocks at velocities of $U = 240\,\mathrm{m/s}$, even though the speed of sound is around $c \approx 310\,\mathrm{m/s}$. Screeching has not been found to have such side effects in previous literature and could pose some complex structural difficulties. Another apparent phenomenon in this set of instantaneous vector fields is how the jet plume undergoes undulations

with high amplitude deflections into the vertical direction. In other words, the jet plume is not stable as is the case with conventional nozzles used on common space launchers.

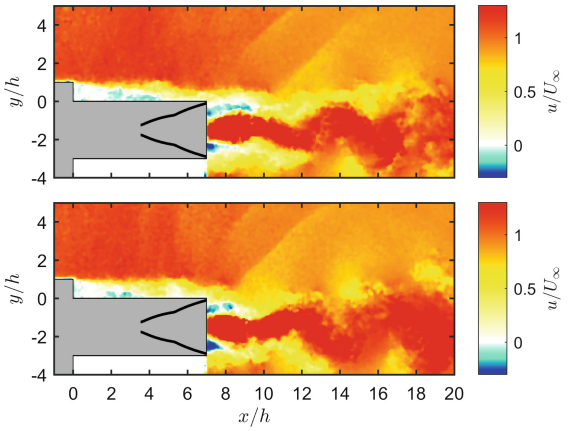

Fig. 4. Illustration of the streamwise component of instantaneous vector fields at $Ma_\infty = 0.8$ with $NPR = 7$

Combining the gathered insights from the instantaneous vector fields with the two-point correlation, one can make certain assumptions about the interaction between the outer flow and the nozzle flow as well as screeching. The strong shock-like acoustical correlations seen around the nozzle systematically merge together with alternating Kelvin-Helmholtz (KH) structures in the proximity of the BFS. These KH structures were identified to be instabilities caused by the step mode in [2]. According to the general knowledge of gas dynamics, the step mode should not be aware of screeching, due to the presence of shocks. Therefore their coherent interaction should be limited. However, the seamless combination of the step mode structures with the screech shocks in the correlation image can be explained by the fact that the shear layer structures stemming off of the BFS influence into which direction the nozzle flow is temporally deflected. The deflection of the nozzle flow then influences the sound waves, or screeching, that are generated at a source further downstream. Thus, a complex interaction between the nozzle flow and the external flow has been established. This causes an unstable jet plume when the Dual-Bell is in sea level mode. Further investigations have to be carried out to see what conditions are conducive to screeching and to see whether the nozzle stability can trigger any negative effects that would make the thrust vectoring on a space launcher more difficult, for example.

3.2 Altitude Mode

In supersonic conditions a strong supersonic expansion occurs around the nozzle's lip. This drastically reduces the static pressure in the vicinity of the nozzle

exit below ambient conditions, effectively increasing the NPR. This static pressure can be referred to as p_{PM} denoting the influence of the Prandtl-Meyer expansion. Thus, during the design phase of a Dual-Bell nozzle the effective nozzle pressure ratio $NPR_{\text{eff}} = \frac{p_0}{p_{PM}}$ has to be considered, in order for transition to occur at the desired condition, especially in supersonic flight conditions. Figure 5 shows the mean flow field when the nozzle is in altitude mode, along with the static pressures present at the various locations. At $Ma_\infty = 2.0$, a supersonic expansion around the BFS, followed by a recompression shock at the reattachment surface overall decreases the static pressure by 10%. Then, the previously noted expansion around the nozzle's lip drastically reduces the static pressure by 58% compared to the free-stream pressure. This makes $NPR_{\text{eff}} = 45.1$, which is more than twice as high as the regularly defined nozzle pressure ratio of $NPR = 18.8$. In contrast to sea level mode, there is no apparent correlation between the nozzle and the outer flow when correlating the fluctuating component of the vertical velocity scalar v', at a location close to the nozzle exit with the rest of the FOV. Also, the dynamics of the nozzle, or the undulations, are not present when the nozzle operates in altitude mode. In other words, the strong interaction between the nozzle and the outer flow only take place during sea level mode. Further investigations need to be carried out, to see whether an interaction would be present if the altitude mode was reached in transonic flight conditions.

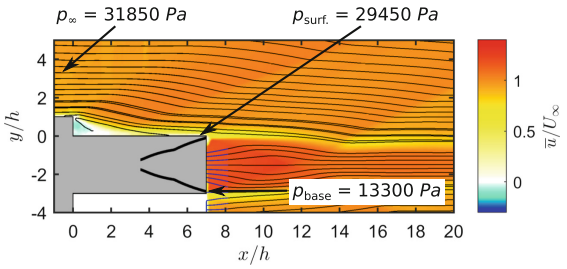

Fig. 5. Illustration of the streamwise component of the mean flow field at $Ma_\infty = 2.0$ with $NPR = 18.8$ ($NPR_{eff} = 45.1$)

3.3 Transition

The transition from sea level to altitude mode occurs relatively sudden. Figure 6 shows the run time of the wind tunnel vs. a nozzle mode criterion, which was defined in the work frame of these experiments. The nozzle mode criterion evaluates the light intensity of each schlieren image in a defined evaluation window close to the nozzle exit (refer to white rectangle in the images of Fig. 7). As the average value of this evaluation window is usually close to either 0 or 1 (sea level or altitude mode) on a normalized scale, it gives very reliable information about the nozzle mode. For reference purposes, two schlieren images are provided in

Fig. 7, displaying the nozzle at sea level and altitude modes, recorded at instances indicated by the asterisks in Fig. 6. During the time frame in between the two asterisks in Fig. 6, two transition events, with one retransition in between, take place. The transition from sea level to altitude mode takes about 0.01 s. The retransition back to sea level mode takes about another 0.01 s, making a period last 0.02 s. If this phenomenon were to occur periodically, this would yield a frequency of around 50 Hz. When looking at the entire time frame in Fig. 6, one can see that from about 0.7 s to 2.7 s into the wind tunnel run, 40 transitions with retransitions, also known as 'flip-flop' events, take place. This is very problematic, especially when considering the relatively fast increase in NPR. It also becomes evident that the range of $NPR = 4.2$–4.4 is very critical for this nozzle. Since retransition can take place throughout such a wide range of NPR, this could indicate that the nozzle has a low hysteresis. However, another possibility is that retransition to sea level mode is triggered by a sudden increase in static pressure surrounding the nozzle exit when the flow expands into the second Bell. Thus, the transition into altitude mode would cause an instant decrease in the Prandtl-Meyer expansion angle around the nozzle's lip, leading to an increased static pressure in the vicinity of the nozzle exit. This local increase in static pressure then decreases NPR_{eff} to the point where the nozzle would naturally be in sea level mode. Now, when the nozzle retransitions back into sea level mode, the Prandtl-Meyer expansion angle around the nozzle's lip instantly increases again, decreasing the static pressure in the vicinity of the nozzle exit. This increases NPR_{eff} back to a value where the nozzle naturally would be altitude mode again. The coupled phenomena of the Prandtl-Meyer expansion angle around the nozzle's lip and the nozzle's mode would also explain the reoccurring flip-flop phenomenon taking place. In order to verify this theory, experiments with a nozzle designed for transitioning in the transonic regime will be carried out. This will yield important information regarding the hysteresis criteria of Dual-Bell nozzles, as well as their feasibility to be used on future space launchers without active control of the transition event.

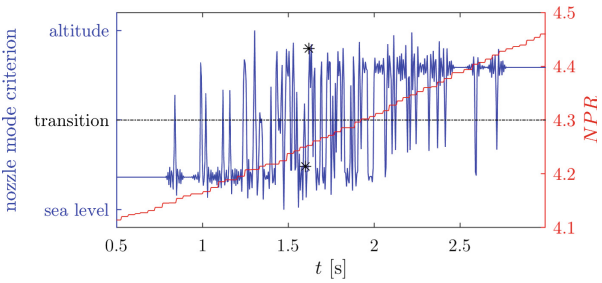

Fig. 6. Time vs. nozzle mode criterion. Asterisks provide the instance of the schlieren images provided in Fig. 7

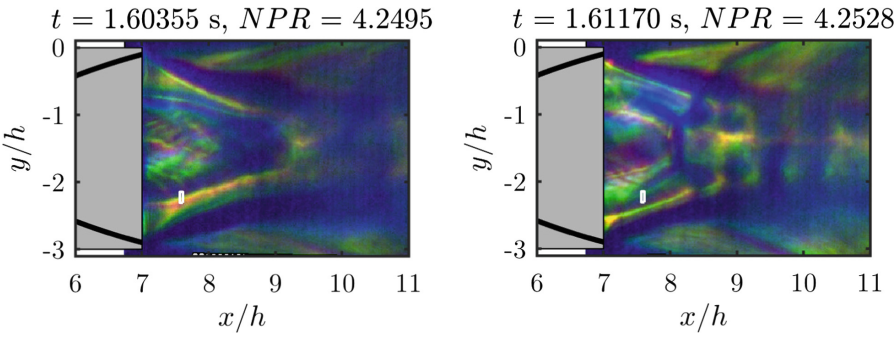

Fig. 7. Schlieren shadowgraph of the nozzle in sea level mode (left) and in altitude mode (right)

4 Conclusions

Experimental measurements on planar Dual-Bell nozzle have been carried out in the TWM at both, transonic and supersonic conditions. Both, the sea level mode as well as the altitude mode can be achieved in this experimental setting, with a broad spectrum of NPRs. Furthermore, the transition from sea level to altitude mode has been captured via 4-color schlieren recordings at 20 kHz. The results in sea level mode show that there is a very strong interaction between the nozzle and the outer flow. Screeching plays a role in this, which transfers information from the nozzle flow upstream and leads to shocks above the reattachment surface. The apparently large dynamics of the jet plume in sea level mode could also lead to nozzle side loads or thrust vectoring difficulties on a real application. Once the nozzle has fully transitioned into the stable regime of the altitude mode, there is no apparent interaction between the nozzle flow and the outer flow. Furthermore, the jet plume is very stable in this mode, not causing any potential thrust vectoring problems. The presence of multiple retransitions over a broad range of NPR is also problematic for the structural integrity of a realistic nozzle. Due to the possible triggering of the flip-flop phenomenon caused by the interaction of the supersonic expansion around the nozzle's lip and the operational mode of the nozzle, a nozzle designed for the transition to occur in the transonic regime could yield more favorable results in the future. Overall, these results show that an external flow has a dramatic influence on the behavior of a Dual-Bell nozzle. Its effects should always be considered for any future investigations.

Acknowledgments. Financial support has been provided by the German Research Foundation (Deutsche Forschungsgemeinschaft – DFG) in the framework of the Sonderforschungsbereich Transregio 40.

References

1. Hannemann, K., Lüdeke, H., Pallegoix, J.-F., Ollivier, A., Lambaré, H., Maseland, J.E.J., Geurts, E.G.M., Frey, M., Deck, S., Schrijer, F.F.J., Scarano, F., Schwane, R.: Launcher vehicle base buffeting - recent experimental and numerical investigations. In: Proceedings 7th European Symposium on Aerothermodynamics for Space Vehicles, vol. 692 (2011)
2. Bolgar, I., Scharnowski, S., Kähler, C.J.: The effect of the mach number on a turbulent backward-facing step flow. Flow Turbul. Combust. **101**(3), 653–680 (2018). https://doi.org/10.1007/s10494-018-9921-7
3. Bolgar, I., Scharnowski, S., Kähler, C.J.: Passive flow control for reduced load dynamics aft of a backward-facing step. AIAA J. **57**(1), 120–131 (2019). https://doi.org/10.25141/1.J057274
4. Stark, R., Génin, C., Schneider, D., Fromm, C.: Ariane 5 performance optimization using dual-bell nozzle extension. J. Spacecraft Rockets **53**(4), 743–750 (2016). https://doi.org/10.2514/1.A33363
5. Foster, C., Cowles, F.: Experimental study of gas-flow separation in overexpanded exhaust nozzles for rocket motors. In: Jet Propulsion Laboratory, California Institute of Technology, Progress Report, pp. 4–103 (1949)
6. Pergio, D., Schwane, R., Wong, H.: A numerical comparison of the flow in conventional and dual bell nozzles in the presence of an unsteady external pressure environment. In: 39th Join Propulsion Conference and Exhibit, Huntsville, AL, USA, AIAA, p. 4731 (2003). https://doi.org/10.2514/6.2003-4731
7. Nürnber-Génin, C., Stark, R.: Flow transition in dual bell nozzles. Shock Waves **19**(13), 265–270 (2009). https://doi.org/10.1007/s00193-008-0176-4
8. Nürnber-Génin, C., Stark, R.: Experimental study on flow transition in dual bell nozzles. Shock Waves **126**(3), 497–502 (2010). https://doi.org/10.2514/1.47282
9. Verma, S.B., Stark, R., Nürnberger-Génin, C., Haidn, O.: Cold-gas experiments to study the flow separation characteristics of a dual-bell nozzle during its transition modes. Shock Waves **20**(3), 191–203 (2010). https://doi.org/10.1007/s00193-010-0259-x
10. Verma, S.B., Stark, R., Haidn, O.: Effect of ambient pressure fluctuations on dual-bell transition behavior. J. Propul. Power **40**(5), 1192–1198 (2014). https://doi.org/10.2514/1.B35067
11. Statnikov, V., Roidl, B., Meinke, M., Schröder, W.: Analysis of spatio-temporal wake modes of space launchers at transonic flow. In: 54th AIAA Aerospace Sciences Meeting (2016). https://doi.org/10.2514/6.2016-1116
12. de Brederode, V., Bradshaw, P.: Three-dimensional flow in nominally two-dimensional separation bubbles: flow behind a rearward-facing step. In: Imperial College, London, Great Britain, Technical Report (1972)
13. Kähler, C.J., Sammler, B., Kompenhans, J.: Generation and control of tracer particles for optical flow investigations in air. Exp. Fluids **33**(6), 736–742 (2002). https://doi.org/10.1007/s00348-002-0492-x
14. Scharnowski, S., Kähler, C.J.: On the effect of curved streamlines on the accuracy of PIV vector fields. Exp. Fluids **54**(1), 1435 (2013). https://doi.org/10.1007/s00348-012-1435-9
15. Scharnowski, S., Kähler, C.J.: Estimation and optimization of loss-of-pair uncertainties based on PIV correlation functions. Exp. Fluids **57**(2) (2016). https://doi.org/10.1007/s00348-015-2108-2

16. Mendez, M.A., Raiola, M., Masullo, A., Discetti, S., Ianiro, A., Theunissen, R., Buchlin, J.-M.: POD-based background removal for particle image velocimetry. Exp. Therm. Fluid Sci. **80**, 181–192 (2017). https://doi.org/10.1016/j.expthermflusci.2016.08.021
17. Hampel, A.: Auslegung, Optimierung und Erprobung eines vollautomatisch arbeitenden Transsonik-Windkanals. In: Hochschule der Bundeswehr, Ph.D. Dissertation (1984)
18. Rodgers, J.L., Nicewander, W.A.: Thirteen ways to look at the correlation coefficient. Am. Stat. **42**(1), 59–66 (1988)
19. Panda, J.: Shock oscillation in underexpanded screeching jets. J. Fluid Mech. **363**, 173–198 (1998). https://doi.org/10.1017/S0022112098008842
20. Alkislar, M.B., Krothapalli, A., Lourenco, L.M.: Structure of a screeching rectangular jet: a stereoscopic particle image velocimetry study. J. Fluid Mech. **489**, 121–154 (2003). https://doi.org/10.1017/S0022112003005032